ECN-W--07-010

The stability of PEMFC electrodes: Platinum dissolution versus potential and temperature investigated by Quartz Crystal Microbalance

V.A.T. Dam

F.A. de Bruijn

Accepted for publication in the Journal of the Electrochemical Society.

January 2007

The stability of PEMFC electrodes: Platinum dissolution versus potential and temperature investigated by Quartz Crystal Microbalance

Van-Anh. T. Dam[1] and Frank A. de Bruijn[1,2,*]

1. Inorganic Chemistry and Catalysis group, Eindhoven University of Technology P.O. Box 513, 5600 MB Eindhoven, The Netherlands

2. Energy Research Centre of the Netherlands (ECN), P.O. Box 1, 1755 ZG, Petten, The Netherlands

* corresponding author. email: debruijn@ecn.nl; fax: +31 224 568489

Abstract

The stability of platinum in PEM fuel cell electrodes has been investigated by determining the dissolution of platinum from a thin platinum film deposited on a gold substrate in 1M $HClO_4$ at different temperatures ranging between 40 and 80°C and potentials between 0.85 and 1.4 V vs. RHE. The loss of Pt during the dissolution process is monitored *in-situ* with the highly sensitive quartz crystal microbalance. By combination of the microbalance with the electrochemical cell, the dynamic change of the electrode weight can be observed *in-situ*. It is shown that first an oxide layer is formed, which can be dissolved depending on temperature and potential.

The dissolution rate is found to be strongly dependent on the potential and temperature. At a potential close to 1.15 V vs. RHE, the dissolution rate becomes saturated at 80°C due to the protection of a passivating surface platinum oxide layer at high potential. At 80 °C, the dissolution rate starts to diminish when the potential is higher than 1.15V.

keywords: platinum; dissolution; PEMFC

Introduction

Degradation of proton exchange membrane fuel cells (PEMFCs) performance has been getting increasing attention for the last couple of years. Among the degradation mechanism, loss of platinum leading to a reduced electrochemically active surface area of the catalyst layers, has been considered as an important cause of loss of fuel cell performance. The Pt loss especially takes place when high electrode potentials occur [1-6], e.g during load cycles, shutdown of the fuel cells or under fuel starvation [7,8].

Loss of platinum can occur due to the oxidation of platinum itself, or due to the corrosion of the carbon support [9]. In either case, the active surface area on which oxygen reduction takes places is reduced. Poisoning of the membrane as a result of platinum diffusion into the proton exchange membrane can take place as well [10].

In highly acidic medium, under the operating voltage, Pt can also be dissolved and then migrates and re-deposits on other Pt particles in catalyst layer to form larger particles (sintering or Ostwald ripening). The mechanism of the Pt dissolution phenomenon has been suggested in detail in [11-13].

Furthermore, the dissolved platinum can also be removed and diffuse to other parts of MEA following the coalescence mechanism [12]. The magnitude of the Pt dissolution and re-deposition phenomenon depends strongly on the fuel cell operating voltage. The influence of potential at low temperatures on the Pt dissolution has been reported by Wang and Kawahara [14,15].

To date, the Pt dissolution has only been studied *ex-situ* by determining the Pt concentration after the dissolution process [14,15]. In this paper we present a different method to directly investigate the dissolution of Pt thin film under potentiostatic condition in 1M $HClO_4$ at different temperatures ranging from 40 to 80°C. By using the conventional electrochemical cell in combination with a quartz crystal microbalance, the weight of the Pt electrode is *in-situ* monitored with high sensitivity during the dissolution process. This method gives an opportunity to investigate in detail the elementary steps of the dissolution mechanism including formation of the surface Pt oxide layer and its further dissolution, thus giving a better insight into dynamics of the Pt dissolution in the fuel cell.

Experimental

A commercial quartz crystal purchased from Maxtex which has a thin polished gold electrode with an area of 1.37 cm^2, was used as a substrate for Pt deposition. Before deposition of Pt, the gold electrode was electrochemically cleaned in 0.5M H_2SO_4 by applying a cycling potential between 0.2 and 1.7 V vs. RHE for at least 30 minutes.

A Pt thin film on the gold electrode was obtained from a mixture of 0.02 mM H_2PtCl_6 and 0.02 M Na_2HPO_4. The film was electrochemically deposited under a constant current regime of 1 mA on the cleaned gold electrode. The thickness of the Pt film varies depending on the deposition time, which was typically between 3-5 minutes.

After deposition, the Pt electrode was rinsed with distilled water to remove the residue of the deposition solution. The electrode was further annealed in 1M $HClO_4$, which is prepared from chloride free $HClO_4$ 70% (Suprapur, Merck) and ultra pure 18 MΩ.cm Millipore water, by applying a cycling potential between 0.05 and 1.3 V vs. RHE for at least 20 cycles to stabilize the morphology and surface state of the Pt electrode. All cyclic voltammograms were performed at a sweep rate of 50mV/s.

The electrochemical cell, which is used for applying a constant potential consists of the deposited Pt electrode as a working electrode, a Pt disk as a counter electrode and a $Hg/HgSO_4$ reference electrode. All electrode potential values in this paper are reported versus the reversible hydrogen electrode (RHE). In this setup the working electrode, which is at the same time an electrode for the microbalance, was separated from the counter electrode by a separate glass membrane. The volume of compartment for the working electrode is about 230ml. Before the experiment, the dissolution solution, 1M $HClO_4$, was purged with purified Argon to remove dissolved oxygen. During experiments, the temperature of the dissolution batch was stabilized and controlled by a thermostat. Before the dissolution experiment, the Pt electrode is subjected to potential cycling between 0.05 and 1.3 V to remove all native oxide on the surface until the electrode cyclic voltammogram becomes unchanged. The cyclic voltammetry is stopped at an end potential of 0.45V, thus the dissolution experiments are started on an oxygen-free platinum surface. The dissolution of the Pt electrode was performed at a constant electrode potential by applying a step potential from 0.45V to the required potential while the electrode weight was simultaneously monitored with the microbalance. The mass of the electrode is set at zero when the dissolution process is started. For each set of measurements done at the same potential, a fresh electrode was prepared. The experiments at the same potential but at different temperatures were measured with the same electrode. Between these experiments, the preconditioning procedure was the same, i.e. potential cycling in order to obtain a clean and reproducible platinum surface.

The time of the dissolution experiment was taken such that the oxide layer build up and dissolution could be measured accurately. Consequently, the measuring times were not the same for all experiments, i.e. much shorter for high temperatures and at the same temperature shorter for higher potentials.

The dissolution was studied in the potential range between 0.85 and 1.4 V at temperatures between 40 and 80°C.

Results

During the platinum deposition on the gold substrate, the total weight of Pt deposited on the electrode linearly increases with deposition time. After 4 minutes of deposition, approximately 63 μg of Pt has been deposited on the gold electrode. After the Pt deposition, a cyclic voltammogram of this electrode is taken in 1M $HClO_4$ and shows only oxidation and reduction peaks of Pt oxide and H-adsorption and desorption on Pt. No peaks for gold and gold oxide are observed.

In Fig.1, dependence of the electrode weight on the applied potential during cyclic voltammetry at a sweep rate of 50 mV/s is plotted. The arrows in the graph show the direction of the sweeping potential. Comparing it with the cyclic voltammogram plotted in the same Fig. 1, it is clear that at a potential higher than 0.45V, the weight of the electrode increases when the Pt oxide layer is formed and decreases when the reduction of the oxide layer occurs. At further potential reduction from 0.45 to 0.05V, the weight of the electrode decreases in spite of hydrogen adsorption occurring. The same phenomenon was observed by Birss et al. [16], who explained this by the desorption of water when the electrode potential is lowered from 0.45 V to 0.05 V. In a potential range close to 0 V, the desorption-adsorption of water at the electrode surface becomes stabilized, the mass of the electrode stays unchanged. The complete desorption of water results in 0.24μg loss in the electrode mass. Upon increase of the potential up to 0.45 V adsorbed water replaces again adsorbed hydrogen.

From the H-adsorption region in the electrode CV, assuming 0.210 mC per "real" cm^2 of Pt [17], the electrode surface area was calculated to be about 24 cm^2. According to the electrode mass change during oxidation by scanning the potential from 0.45 to 1.3V, each surface platinum atom is covered by 0.44 O atoms, using 1.31×10^{15} atoms per cm^2 for the density of platinum atoms on polycrystalline Pt surface [17]. This surface coverage is lower than that calculated from the coulombs passed to reduce the oxide, which amounts to 0.54 O atoms per surface platinum atom.

The mass changes of the Pt electrode during the dissolution process under potentiostatic condition, in 1M $HClO_4$ at 80°C are presented in Figure 2.

Figure 2A shows the change in the mass of the working electrode for the experiment at 0.85V and 80°C. Two regions can clearly be discerned. In the first 150 minutes, the mass of the electrode increased up to a certain maximum. The gain in the electrode mass is much higher than that can be obtained from the water adsorption (see Fig. 1). After these 150 minutes, the mass started to decrease, while the electrode potential was maintained. The decrease rate of the mass remained almost constant for a long period of time.

A similar increase of mass followed by a decrease was also observed at higher dissolution potentials. In Fig. 2B-E, measured changes in electrode weights at dissolution potentials ranging from 0.95 to 1.4 V are plotted. Measuring time of these experiments is varied depending on how fast the dissolution occurs. As can be seen in these figures, both the rate of increase of the mass as well as the rate of decrease is accelerated with increasing the electrode potential. Comparison of data in Figure 1 and 2 strongly suggests that the mass increase is a result of net oxide formation, whereas the decrease can be related to net dissolution. The oxidation of Pt can proceed according to [18]:

$$Pt + H_2O \leftrightarrow PtO + 2H+ + 2e^- \qquad E_0 = 0.98 - 0.059 \text{ pH} \qquad (1)$$

$$PtO + H_2O \leftrightarrow PtO_2 + 2H^+ + 2e^- \qquad E_0 = 1.05 - 0.059 \text{ pH} \qquad (2)$$

Depending on the potential, PtO and PtO_2 are formed resulting in an increase of the electrode mass as seen in the oxidation region of Fig. 2A-E. The rate of the oxide layer formation depends on the applied potential. Pt dissolution can occur via the dissolution of the surface oxide layer or even from metallic platinum as follows:

$$PtO + 2H^+ \leftrightarrow Pt^{2+} + H_2O \qquad \log [Pt^{2+}] = -7.06 -2 \text{ pH} \qquad (3)$$

$$PtO_2 + 4H^+ + 2e^- \rightarrow Pt^{2+} + 2H_2O \qquad E_0 = 0.84 - 0.12 \text{ pH} -0.03 \log [Pt^{2+}] \qquad (4)$$

$Pt \leftrightarrow Pt^{2+} + 2e^{+}$ $\quad\quad$ $E_0 = 1.12 + 0.029 \log [Pt^{2+}]$ $\quad\quad$ (5)

Assuming a Butler-Volmer relation between the equilibrium potential and the reaction rate for reactions 4 and 5, the Pt dissolution rate strongly depends on the potential and concentration of Pt ions in solution. When the dissolution time is long enough, the dissolution process can be inhibited due a rising of the equilibrium concentration of Pt in solution, which is typically observed at the dissolution curve at 0.95V (see Fig. 2B). The maximum mass measured at a certain condition is the result of the mass increase due to oxide formation and the loss of mass caused by its dissolution. The fact that the mass maximum does not continuously increase with increasing potential shows that the mechanism of oxide growth and dissolution is rather complex. The mass change is thus a combination of mass increase due to oxide layer growth and a mass decrease due to dissolution. As the exact mechanism is unknown, no corrections have been made in the reported dissolution rates, by taking into account these simultaneous phenomena.

In Fig. 2F, the steady state current at the electrode during dissolution at 1.4V is plotted. The charge transfer in the cell during 30 minutes calculated from this curve in the dissolution region in Fig. 2F is estimated to be about 19.43 mC. The measured amount of dissolved platinum amounted to 7.29 μg as shown in Fig. 2E. According to Faraday's law and assuming a reaction with two electrons involved, this amount of mass change would correspond to a charge of 7.21 mC, which is much lower than the actual number of 19.43 mC. It means that platinum oxide is still formed during its dissolution. Even if the dissolution of platinum is a 4 electron process, i.e. PtO_2 dissolves as Pt^{4+}, still more charge is passed. In case platinum dissolves from its platinum oxide, a new layer of oxide is formed subsequently.

When the dissolution temperature was lowered to 60°C, the whole dissolution process happened at a lower rate. At a potential of 0.85V, only an increase of the electrode mass was observed without subsequent decrease. For the dissolution temperature of 40°C, even at a potential of 1.2V, no dissolution was observed after 90h (see Fig. 3). Therefore it can be concluded that the Pt dissolution can only occur under a favorable condition which is a combination of oxide layer thickness, temperature and potential. While the thickness of the oxide layer is a result of the potential and the duration of the exposure to this potential and temperature, the rate of dissolution of this oxide layer depends on temperature and potential as well.

Just after finishing the dissolution process at 60°C as described above, the cyclic voltammogram of the electrode, which starts from a potential of 1.0V and scans negatively, is immediately taken. Irrespective of the potential at which the dissolution was measured, the scan in negative direction was started at 1.0V, to be able to compare the different reduction charges. As the time of the dissolution experiment depended on the dissolution rate, the data shown in Figure 4 are illustrative for the oxide present after dissolution. It does not enable a direct insight in the dependence of oxide layer thickness versus potential. The CV taken after 22h of dissolution at 1.25V shows a huge oxide reduction peak (Fig. 4A). It again confirms that the surface oxide layer is still present and is continuously formed during the dissolution. The surface oxide layer becomes thinner resulting in a smaller oxide reduction peak as the second CV is done.

Comparing the first CVs which are taken after the dissolution experiments at 1.05, 1.15 and 1.25V at 60°C and generated from the same starting potential of 1.0V, the higher the dissolution potential, the larger the oxide reduction peak is seen (Fig. 4B). The increase in the Pt oxidation peaks is also observed in the same order. From data presented in Fig. 4A and B, the number of surface platinum oxide layers present on the electrode before and after taking 1,2 and 5 cyclic voltammograms is calculated and shown in Fig. 4C. It shows that during the dissolution, the surface oxide layer in the Pt electrode is thicker when a higher electrode potential is applied. During the dissolution at a potential lower or close to 1.15V, the electrode is covered with a mono layer of PtO. This oxide layer can partly be removed by applying one potential cycling. When the dissolution potential increases up to 1.25V, more than two PtO layers are found on the electrode surface. Based on our experiments, no distinction can be made between a single layer of PtO_2 or two layers of PtO. The formation of a full monolayer of PtO corresponds to 0.42 $mC.cm^{-2}$ Pt. As the electrode surface was 24 cm², 10 mC of charge will be passed for complete coverage of our electrode with PtO. Adding to this the charge corresponding to the mass change resulting from platinum dissolution (7.3 µg, 7.21 mC), and comparing it to the total charge measured during dissolution, 19.4 mC, and the fact that after a dissolution experiment more than a full monolayer of PtO layer can be reduced, the dissolution is very likely a two electron process, as otherwise a even higher charge should has been measured.

From data such as presented in Figure 3 the dissolution rate of the Pt electrode at different potential and temperature of 60°C and 80°C was calculated from the slope of the decreasing part of the mass-time curve. The results are displayed in Fig. 5 and Table 1. At the temperature of 40°C, the data is not available because only the oxidation is observed.

The logarithm of the dissolution rate was found to increase linearly with increasing potential up to 1.15V. The dissolution rate increased about 54 times as the potential increased from 0.85 to 1.15V. However at 80°C, the dissolution rate reached a maximum at a potential close to 1.15V. It also can be predicted by the data presented in Fig. 4C, which is explained by a presence of the platinum oxide layer. The platinum surface becomes more passive by the oxide layer when the potential reaches 1.15V. When the potential increases further, Pt will be fully protected by platinum oxide [19]. The thickness of the protecting platinum oxide increased sharply above 1.15 V as shown in Fig. 4C. Therefore the dissolution rate decreases at potentials higher than 1.15V as observed in Fig. 5. All measured dissolution rates shown in Fig. 5 are summarized and presented in Table I.

The data of our experiments seem to be in good agreement with the model of Darling and Meyers [20], who calculated the build-up of platinum oxide and the dissolution of platinum for linear sweep experiments. Exact comparison is difficult as our measurements are at constant potential.

Note that the dissolution rates in Table I should be compared to the amount of Pt deposited on the gold substrate, which is typically between 63 to 80μg. Taking the dissolution rate at 1.15V and 80°C, the electrode with a mass of 63 μg can completely be dissolved after 1hour 40 minutes yielding a platinum concentration of 1.4 μM. In comparison with previously published results on bulk Pt dissolution [14], which reports the potential dependence of the Pt concentration resulting from platinum dissolution, the obtained data on the dissolution rate presented in Table I have a similar potential dependence. The dissolution rate reported by Wang et al. [14] at 0.9 V and 23 °C, 1.4 10^{-14} $g.cm^{-2}.s^{-1}$ is the same as that reported in Table 1 at 0.95 V and 60 °C, which translates into 1.5 10^{-14} $g.cm^{-2}.s^{-1}$. Although our method is different from that of Wang et al., comparison of the two numbers would lead to the conclusion that especially at temperatures higher than 60°C, the dissolution rate increases dramatically.

As stated before, the mass change is a combination of mass increase due to oxide layer growth and a mass decrease due to dissolution. The reported dissolution rates can in fact be larger than reported in this paper.

Conclusions

To our knowledge, this paper shows for the first time a dynamic method to estimate the dissolution rate of the Pt thin film during potentiostatic condition at elevated temperature by combining the conventional electrochemical setup with a quartz crystal microbalance.

Besides information obtained from the electrochemical measurements, this method allows the *in-situ* observation of the dynamic change of the electrode weight. It can differentiate the oxidation and dissolution during the real-time Pt dissolution. For that reason this technique gives extra advantages in comparison with previously presented techniques in literature, where the dissolution rate is only determined *ex-situ*.

By using this technique, the Pt dissolution in 1M $HClO_4$ during potentiostatic condition has been investigated at different potentials and temperatures. The dissolution rate was found to be strongly dependent on the dissolution potential and temperature according to the Nernst equation. The dissolution was accelerated with increasing of temperature. At the dissolution temperature of 80°C and potential higher than 1.15 V, the observed saturation of the dissolution rate is considered to be due to the protected surface platinum oxide at high potential. A reduction in the dissolution rate has been observed at the dissolution potential close to 1.4V. The dissolution rates found for the thin film Pt are higher than that previously published on bulk Pt dissolution, due to its surface and thin film nature. Due to the characteristics of the electrode used in this study with high surface roughness and thin film nature, the data are relevant for dissolution rates for PEM fuel cell catalysts.

Acknowledgements

This work was part of the Dutch EOS-LT PEMLIFE project, supported by SenterNovem, contractnr. EOSLT01029.

References

1. Y. Shao-horn, P.J. Ferreira, G.J. la O', R. Makharia, S. Kocha and H. Gasteiger, Sym. on Durability and reliability of low-T Fuel cell and Fuel cell systems, Los Angeles, Oct. 16-21 (2005).

2. J. Yu, T. Matsuura, Y. Yoshikawa, N. Islam, and M. Hori., Electrochem. and Solid State Let., 8 (3), A156-A158 (2005).

3. D. Liu, and S. Case, J. Power Sources, 162 (1) 521 -531 (2006).

4. J. Xie, D. L. Wood III, D. M. Wayne, T. A. Zawodzinski, P. Atanassov, R. L. Borupa, J. of the Electrochem. Soc., 152 (1), 104-113 (2005).

5. J. Xie, D. L. Wood III, K. L. More, P. Atanassove, R. L. Borup, J. of the Electrochem. Soc., 152 (5), 1011-A1020 (2005).

6. S. J. C. Cleghorn, D. K. Mayfield, D. A. Moore, J. C. Moore, G. Rusch, T. W. Sherman, N. T. Sisofo, and U. Beuscher, J. Power Sources 158 (1), (2006).

7. S. D. Knights, K. M. Colbow, J. St-Pierre, and D. P. Wilkinson, J. Power Sources 127, 127-134. (2004).

8. A. Taniguchi, T. Akita, K. Yasuda, and Y. Miyazaki, J. Power Sources, 130, 42-49 (2004).

9. Y. Shao, G. Yin, Y. Gao, and P. Shi, J. of the Electrochem. Soc., 153, 1093-1097 (2006).

10. Y. Shi, A. Horky, O. Polevaya, and J. Cross, Washington, Courtesy Associates, Fuel Cell Seminar Abstracts, 2005.

11. Z. Nagy and H. You, Electrochim. Acta, 47, 3037-3055 (2002).

12. P. J. Ferreira, G. J. la O', Y. Shao-Horn, D. Morgan, R. Makharia, S. Kocha, and H. A. Gasteiger, J. of the Electrochem. Soc., 152, 2256-2271 (2005).

13. D.C. Johnson, D.T. Napp, S. Bruckenstein, Electrochim. Acta, 15, 1493-1509 (1970)

14. X. Wang, R. Kumar, and D. J. Myers, Electrochem. and Solid State Let., 9, 225-227 (2006).

15. S. Kawahara, S. Mitsushina, K. Ota, N. Kamyia, Electrochem. Soc. Trans., 3, 1, 625-631 (2006).

16. V.I. Birss, M.Chang, and J. Segal, J. Electroanal. Chem. 355 (1993) 181-191.

17. S. Trasatti and O. A. Petrii, J. Electroanal. Chem., 327, 353 – 376 (1992).

18. M. Pourbaix, Atlas of Electrochemical Equilibrium in Aqueous Solutions, 1st ed., Pergamon Press, New York, 1966.

19. G. Jerkiewicz, G. Vatankhah, J. Lessard, M. P. Soriaga, and Y. S. Park, Electrochim. Acta, 49, 451-1459 (2004).

20. R.M. Darling, J.P. Meyers, J. of the Electrochem. Soc., 150, A1523-1527 (2003).

Table I

Potential vs. RHE (V)	60°C (ng/h.cm^2)	80°C (μg/ h.cm^2)
0.85		0.03
0.95	0.05	0.10
1.05	0.45	0.22
1.15	0.87	1.58
1.25	2.09	-
1.40	-	0.60

List of captions

Figure 1: Dependence of the electrode weight on the applied potential during cyclic voltammetry in 1M $HClO_4$ with sweep rate of 50mV/s.

Figure 2: Time dependence of the electrode weight measured in 1M $HClO_4$ and at 80°C, at different dissolution potentials: 0.85 (A), 0.95 (B), 1.05 (C), 1.15 (D) and 1.4 (E); Time dependence of the steady state current during dissolution at a potential of 1.4V (F).

Figure 3: Time dependence of the electrode weight measured in 1M $HClO_4$ at 40°C and 1.2V.

Figure 4: Cyclic voltammograms of the Pt electrode, which start at a potential of 1.0V and scans negatively, after dissolution at potentials of 1.25V (A), 1.05, 1.15 and 1.25V (B) at 60°C; Number of surface platinum oxide layers after taking 1, 2 and 5 cyclic voltammograms, depends on dissolution potentials (C).

Figure 5: Pt dissolution rate versus dissolution potential and temperature. The real surface area of the electrode is 24 cm^2.

Table I: Platinum dissolution rate per square centimeter of electrochemically active surface area versus potential and temperature.

List of figures

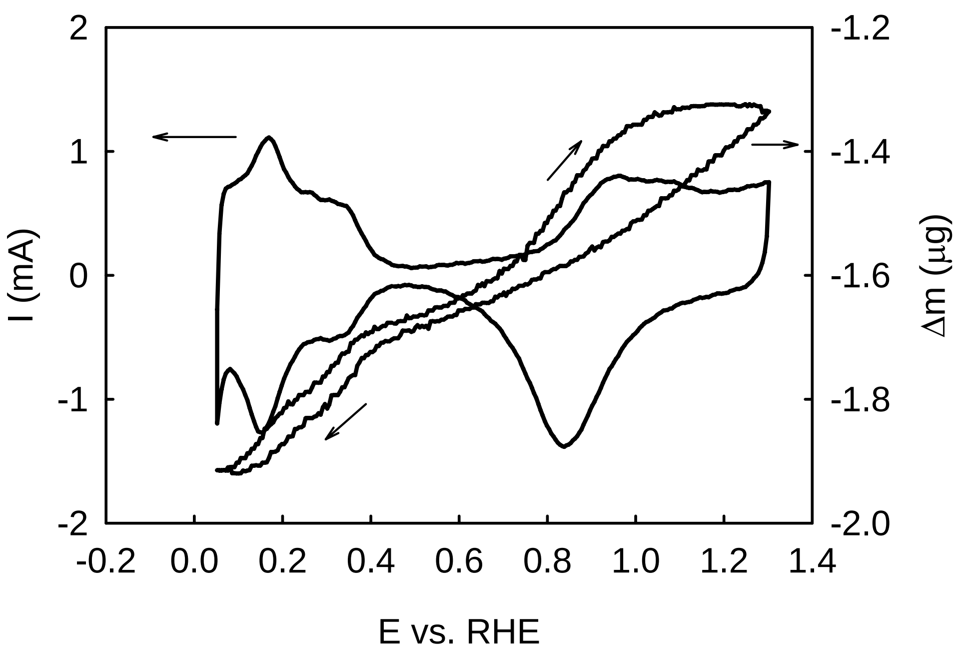

Figure 1

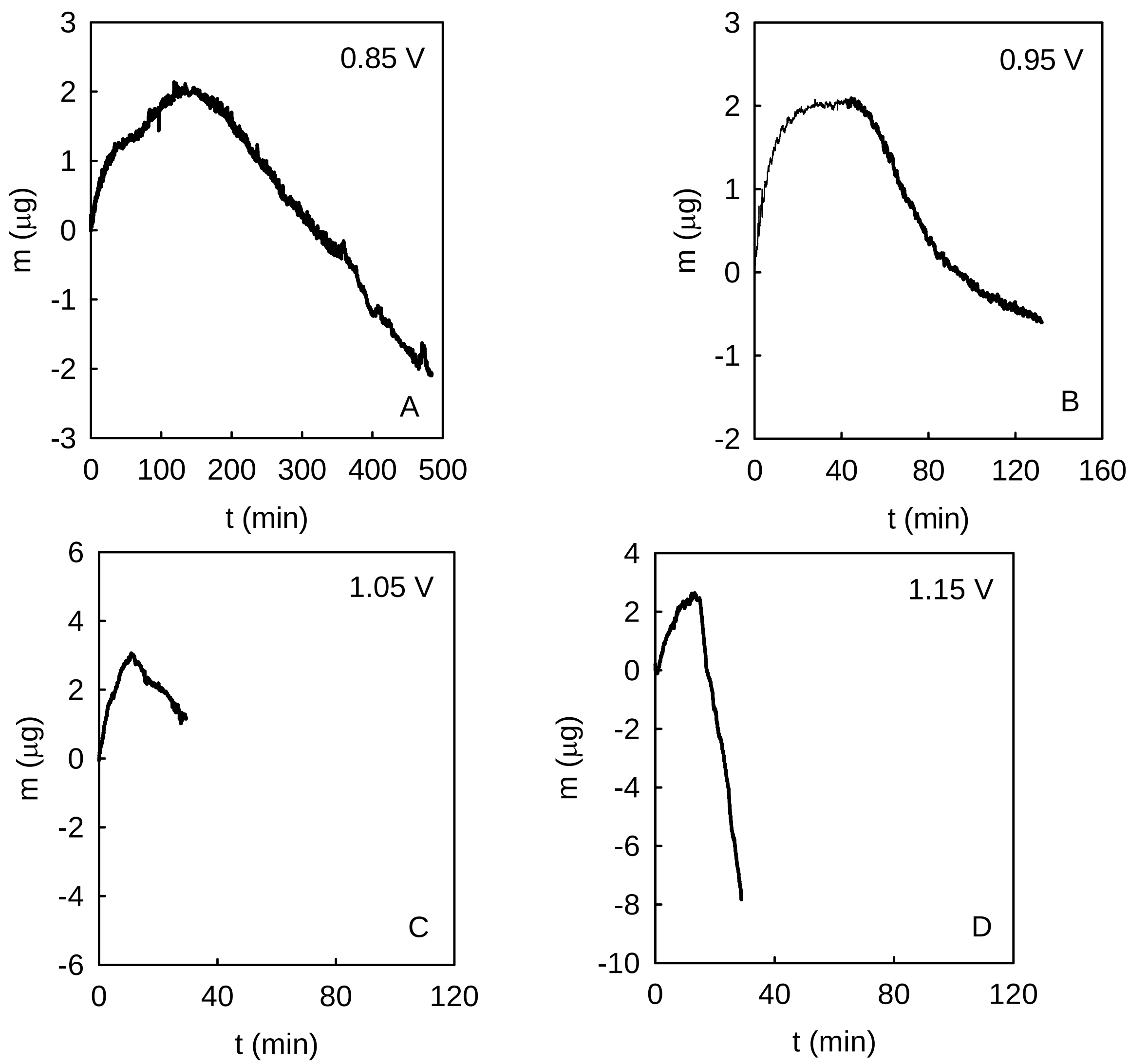

0.85 V
A
0.95 V
B
1.05 V
C
1.15 V
D
m (μg)
t (min)

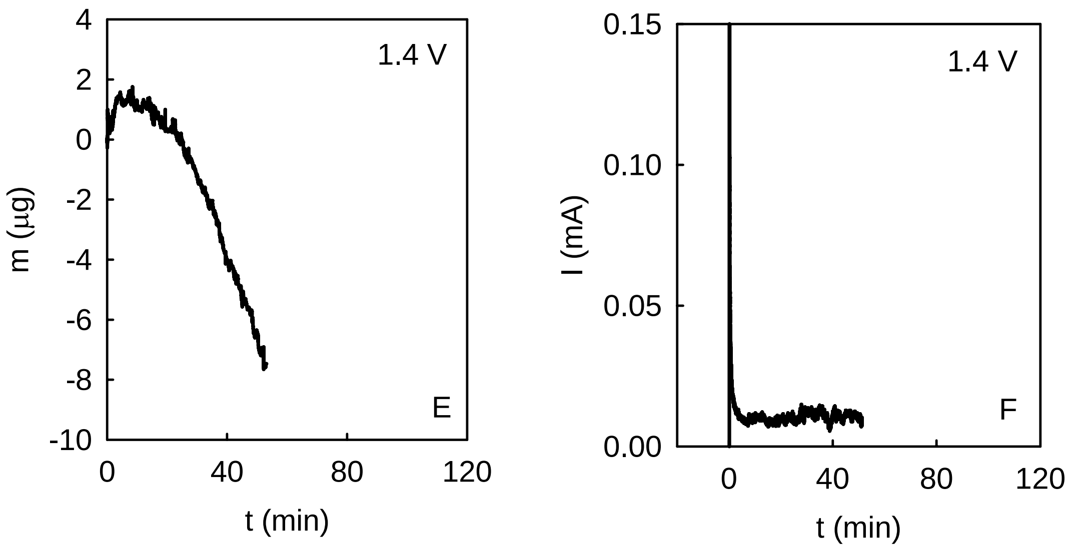

Figure 2

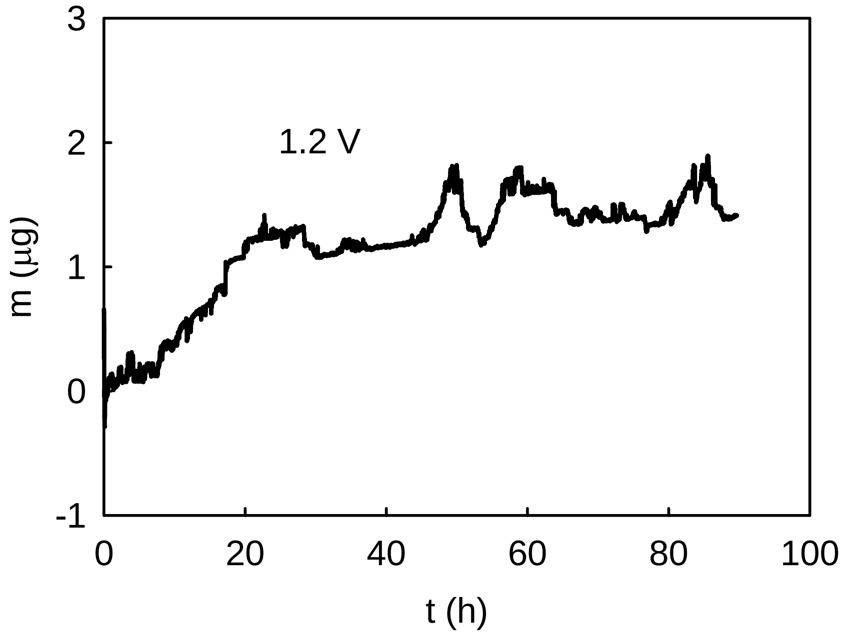

Figure 3

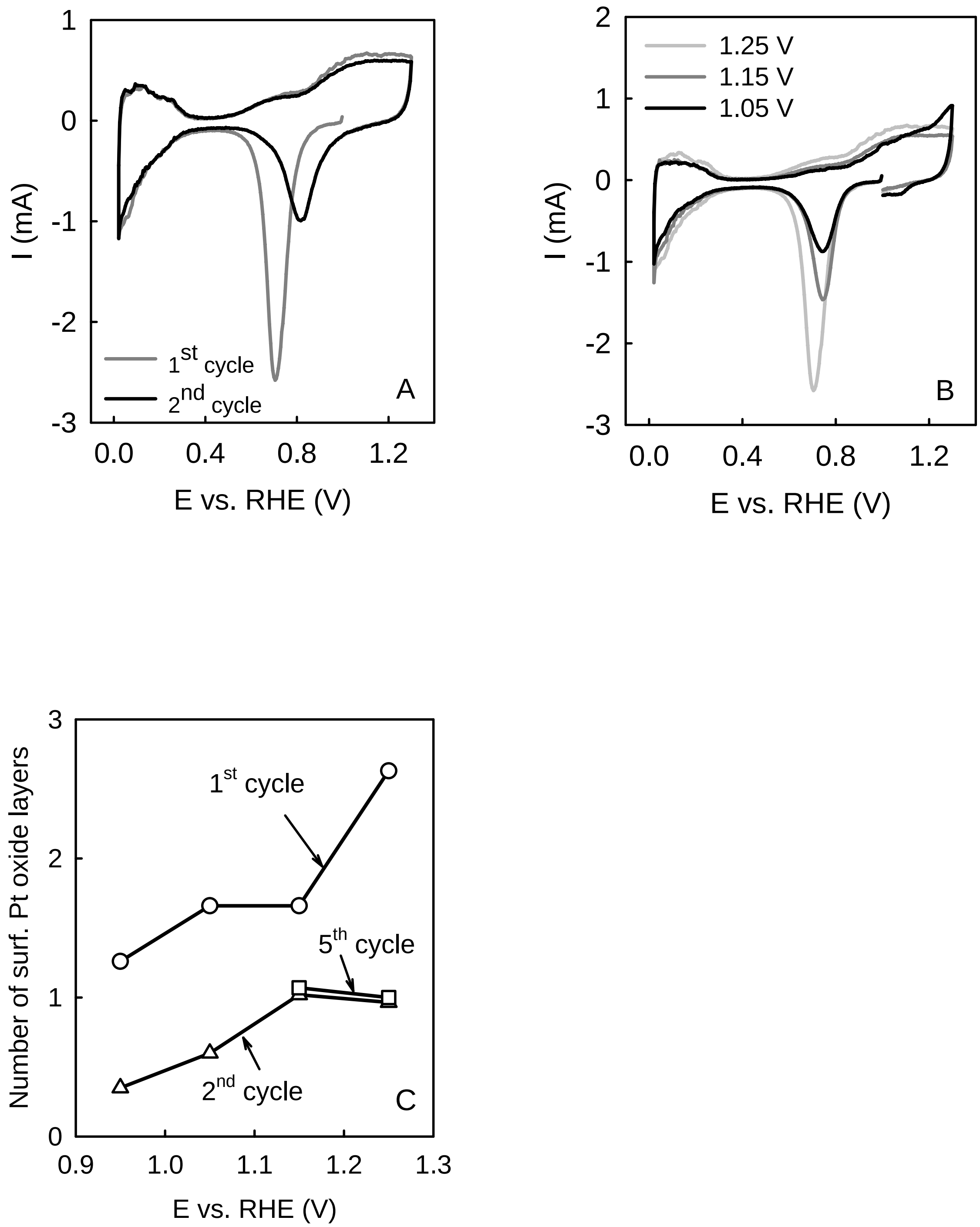

1
0
-1
-2
-3
I (mA)
0.0
0.4
0.8
1.2
E vs. RHE (V)
1st cycle
2nd cycle
A
2
1
0
-1
-2
-3
I (mA)
1.25 V
1.15 V
1.05 V
0.0
0.4
0.8
1.2
E vs. RHE (V)
B
3
2
1
0
Number of surf. Pt oxide layers
1st cycle
5th cycle
2nd cycle
C
0.9
1.0
1.1
1.2
1.3
E vs. RHE (V)

Figure 4

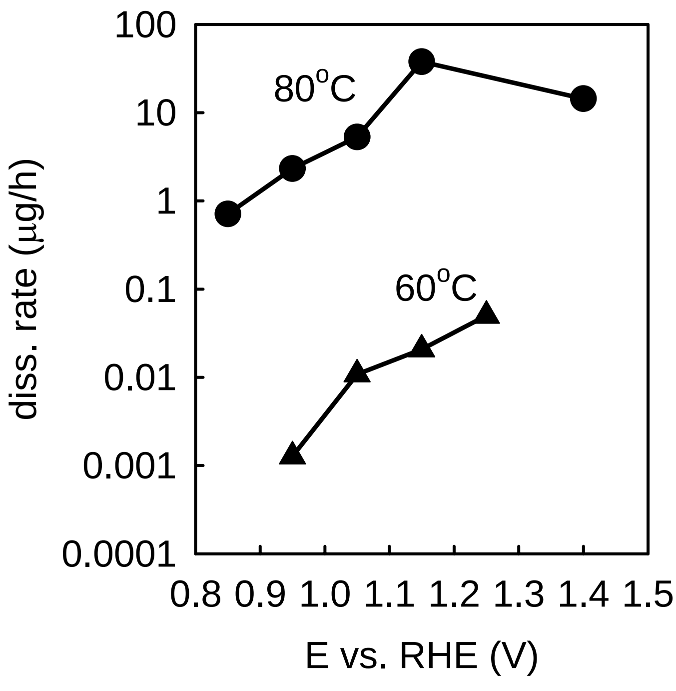

Figure 5

Table I

Potential vs. RHE (V)	60°C (ng/h)	80°C (μg/h)
0.85		0.71
0.95	1.28	2.32
1.05	10.8	5.29

1.15	20.8	37.80
1.25	50.1	-
1.40	-	14.35